Raman study of phonon modes in bismuth pyrochlores

D. J. Arenas,[1,2] L. V. Gasparov,[1] Wei Qiu,[3] J. C. Nino,[3] Charles H. Patterson,[4] and D. B. Tanner[2]
[1]*Department of Physics, University of North Florida, Jacksonville, Florida 32224, USA*
[2]*Department of Physics, University of Florida, Gainesville, Florida 32611, USA*
[3]*Department of Materials Science and Engineering, University of Florida, Gainesville, Florida 32611, USA*
[4]*School of Physics, Trinity College Dublin, Dublin 2, Ireland*
(Received 10 July 2010; revised manuscript received 19 November 2010; published 21 December 2010)

The Raman spectra of the cubic bismuth pyrochlores $Bi_{3/2}Zn_{0.92}Nb_{3/2}O_{6.92}$, $Bi_{3/2}ZnTa_{3/2}O_7$, $Bi_{3/2}MgNb_{3/2}O_7$, and $Bi_{3/2}MgTa_{3/2}O_7$ have been measured at room temperature. The frequencies of the Raman modes, obtained from first-principles calculations, for $Bi_2Ti_2O_7$ are presented for comparison. The spectra of the four samples are similar and agree well with the first-principles calculations. Each bismuth pyrochlore shows more than the six modes expected for the ideal pyrochlore structure. The analysis shows that many of the additional modes could be explained as the relaxation of the selection rules due to the displacive disorder. The Raman modes are assigned by reference to spectra of other pyrochlore materials, comparison to infrared data, and the *ab initio* calculations.

DOI: 10.1103/PhysRevB.82.214302 PACS number(s): 78.30.−j, 63.20.−e

I. INTRODUCTION

Bismuth pyrochlores have been extensively studied for dielectric applications,[1] and have earned recent attention for high-frequency filter applications thanks to their low loss, high permittivity, and good temperature stability.[2] Their pyrochlore structure is described as consisting of interpenetrating networks of BO_6 octahedra and A_2O' chains[3] and it is assigned to the space group $Fd3m$. The nominal composition can be written as $A_2B_2O_7$ or as $A_2B_2O_6O'$ with the latter formula differentiating the oxygen in the A_2O' chains. The pyrochlore family is fascinating because the A and B sites can be occupied by a broad range of elements that can give rise to a great variety of physical properties. In the bismuth pyrochlore, $Bi_{1.5}Zn_{0.92}Nb_{1.5}O_{6.92}$ (BZN), the A site is mostly occupied by Bi and the B site by Nb; while Zn partially occupies both sites. It is important to note that in the literature, cubic BZN is typically described as having the expected nominal composition of $Bi_{1.5}Zn_{1.0}Nb_{1.5}O_7$. However, phase refinement studies,[4] have demonstrated partial substitution of Zn in the A_2O' network (with a resulting oxygen deficiency as presented above) to satisfy the crystallochemical balance between ionic bonding, lattice strain, and charge balance.

The BZN structure has been shown to differ from an ideal pyrochlore structure through random displacements of the A and O' ions.[4,5] This disorder has been attributed to the active lone pair of the Bi cation[6] and appears in the infrared (IR) spectrum of BZN as additional modes from those predicted by the ideal pyrochlore structure.[7–9] The additional IR modes were also observed by Chen *et al.*[7] in three other bismuth pyrochlores $Bi_{3/2}ZnTa_{3/2}O_7$ (BZT), $Bi_{3/2}MgNb_{3/2}O_7$ (BMN), and $Bi_{3/2}MgTa_{3/2}O_7$ (BMT). Here, we present complementary Raman measurements and mode assignments for BMN, BMT, BZN, and BZT; the four ceramics materials studied by Chen *et al.*[7] Both Raman and IR spectroscopy are needed for a more complete picture of the vibrational modes. IR spectroscopy detects only vibrations with a net change in dipole moment and Raman detects those with a net change in polarizability. Furthermore, the Raman study of the pyrochlore structure is useful for a system where different substituents can occupy the A and B sites (such as BZN and the other samples). For the ideal pyrochlore structure, the Raman modes involve movement of oxygen ions only while some IR modes involve motion of the A or B ions.[10] For BZN, the mass difference between Zn and Nb (or Zn and Bi) can lead to splitting of an IR vibrational mode.[7] This is also true for the other three compounds studied here. Also, systematic changes in the IR frequencies across different samples could be attributed to both the changes in the cation's mass and the changes in force constants. In the Raman spectra, however, any systematic differences in frequency are explicitly related to the differences in the force constants for different substituents. The observation of splitting of modes would then suggest appreciable difference in force constant for different substituents in the A and B sites.

There are two main purposes to this work. One is to compare the Raman spectra of bismuth pyrochlores to the vibrational frequencies predicted by first-principles calculations for similar pyrochlores. In this work, we present the frequencies of the Raman modes for $Bi_2Ti_2O_7$ from *ab initio* calculations. The spectra of BMN, BMT, BZN, and BZT agree well with the calculations. This is also true when our spectra are compared to *ab initio* work in the literature on the niobate pyrochlore $Cd_2Nb_2O_7$.[11] The second purpose is to compare the behavior of the Raman-active modes among four bismuth pyrochlores with different substituents and to compare them with the reported spectra of other pyrochlores. The results showed that the Raman spectra are on balance quite similar for the bismuth samples. Each sample showed more than six Raman bands whereas six modes is the prediction for the ideal pyrochlore structure. The appearance of the additional Raman bands, which correspond to Raman-inactive modes of the ideal pyrochlore structure, confirms the displacive disorder of the A and O' sites in the bismuth pyrochlores. The Raman modes were assigned by reference to the Raman spectra of many other pyrochlores,[10–29] some of which include lattice-dynamical calculations,[12,27,28] and first-principles calculations.[11] In the literature, the lattice dynamical and *ab initio* calculations show an interesting difference.

The lattice-dynamical calculations for the Mn and Ti pyrochlores, which use experimental IR and Raman data, are reported to work only when modes observed above 600 cm^{-1} are assumed to be overtones.[12] For $Cd_2Nb_2O_7$, the first-principles calculations by Fischer *et al.*[11] predict a fundamental mode F_{2g} with a frequency as high as 880 cm^{-1}. Our calculations for $Bi_2Ti_2O_7$ also predict a fundamental mode with frequency above 700 cm^{-1}. All four Bi pyrochlores have a mode at 780 cm^{-1} with an intensity higher than most fundamentals. As discussed below, the high intensity of this mode, uncharacteristic of a second-order scattering process, presents interesting questions about these systems.

In the assignment of the modes, it was also considered that the displacement disorder in these samples lowers the symmetry of the system and can result in the relaxation of the selection rules. These displacements of the *A* and O′ sites could make predicted Raman-inactive modes (including IR F_{1u} modes) appear in the Raman spectra. Our computational work for $Bi_2Ti_2O_7$, and the work for $Cd_2Nb_2O_7$ by Fischer *et al.*[11] for a disorderless pyrochlore structure, can give the frequencies of the Raman and infrared modes, as well as some optically inactive modes. The comparison between the Raman data, the IR, and the computational work shows that most of the additional modes observed in the studied here pyrochlores can be attributed to relaxation of the selection rules. Finally, the fact that Zn shares the *A* site with Bi and the *B* site with Nb in BZN did not have a considerable effect on the spectrum of this pyrochlore. There were no additional bands that were attributed to splitting due to different force constants. This was also true for the other three bismuth pyrochlores.

II. EXPERIMENTAL PROCEDURES

Disk-shaped samples, (of 1 cm radius and 5 mm thickness) were prepared by conventional solid-state powder processing techniques.[30] The samples were polished and appeared light yellow. Room-temperature Raman spectra were measured with a T 64000 Jobin Yvon triple Raman spectrometer equipped with a liquid-nitrogen-cooled back-illuminated charge coupled device detector. We used the 488 and 501.7 nm lines of the Ar^+ ion laser to excite Raman scattering. The measurements were done in the subtractive mode[31] with the laser power on the sample not exceeding 6 kW/cm^2 and with an accumulation time of 20 s. The spectra were taken in the back scattering geometry; the scattered light was not polarized while the incident light had vertical polarization.

Phonon calculations at the Γ point of the Brillouin zone were performed for $Bi_2Ti_2O_7$ using a Perdew-Wang approximation[32] to the generalized gradient approximation of density-functional theory using the CRYSTAL code.[33] The *Fd3m* cubic cell containing 22 ions was used. In common with previous calculations for the pyrochlore,[34,35] we find that the high-symmetry cubic structure is unstable with respect to a lattice distortion. Three modes, of F_{1u}, E_u, and F_{2u} symmetry, are found to have imaginary frequencies for the cubic structure. However, none of the Raman-active modes have imaginary frequencies. Further details of the lattice distortions and additional IR-active modes which result when an 88 ion unit cell is relaxed without symmetry constraints are reported elsewhere.[36]

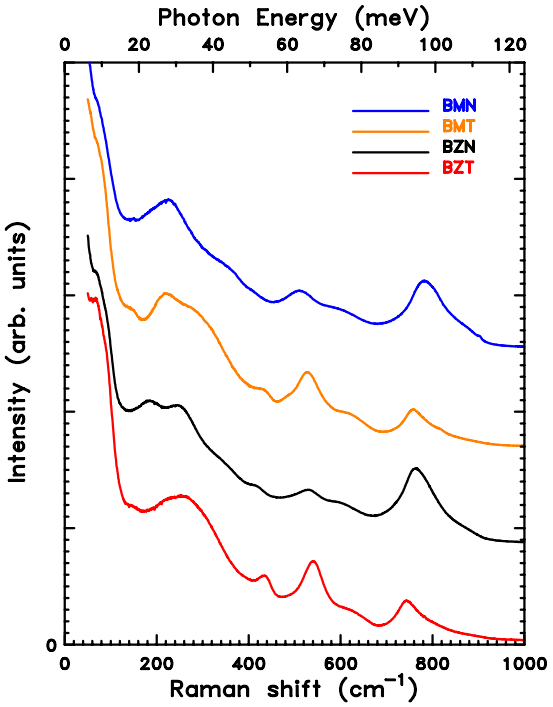

FIG. 1. (Color online) Raman spectra of BMN, BZN, BMT, and BZT. Their intensities have been scaled (by 1, 1.14, 1.64, and 2.46, respectively) and shifted for ease of comparison.

III. RESULTS AND DISCUSSION

A. Analysis of $\chi''(\omega)$

The room-temperature Raman spectra of BMN, BMT, BZN, and BZT are shown in Fig. 1 with scaled and shifted intensities for ease of comparison. The spectra of all four samples were analyzed by solving for the imaginary part of the Raman susceptibility, $\chi''(\omega)$, which is related to the Raman scattering cross section, $\delta^2\sigma/\delta\Omega\delta\omega$, and the Bose factor, $n(\omega)+1$, by the equation

$$\frac{\delta^2\sigma}{\delta\Omega\delta\omega} \propto [n(\omega)+1]\chi''(\omega), \tag{1}$$

where $n(\omega)$ is the Bose-Einstein distribution

$$n(\omega) = \frac{1}{e^{\hbar\omega/k_bT}-1}. \tag{2}$$

Equations (1) and (2) show that the scattering cross section increases rapidly at energies lower than k_bT. For low frequencies, the $1/\omega$ dependence of the Bose factor affects not only the intensity of each mode but also the location of the peak. Therefore, the analysis in this region is improved by dividing the Raman spectra by the Bose factor, $n(\omega)+1$, and obtaining the imaginary part of the Raman susceptibility $\chi''(\omega)$. To study each mode, the imaginary part of the Raman susceptibility can be modeled using a sum of Lorentzian functions

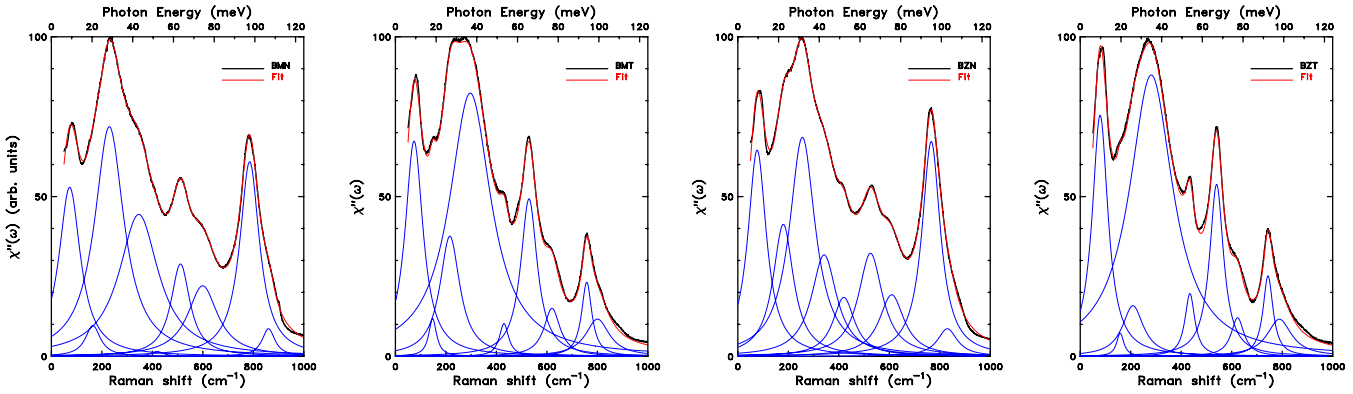

FIG. 2. (Color online) Raman spectra corrected by a Bose factor for our four samples (left to right: BMN, BMT, BZN, and BZT). The obtained imaginary part of the Raman susceptibility was fitted to a sum of Lorentzian functions: $\Sigma A_j/[1+4(\omega-\omega_{oj})^2/\gamma_j^2]$. The figure shows the data (black), the fitting (red), and the individual functions (blue) from the fit.

$$\chi''(\omega) = \sum_j^n \frac{A_j}{1 + \frac{4(\omega - \omega_{oj})^2}{\gamma_j^2}}, \tag{3}$$

where each band has three parameters: a maximum A_j, a center frequency ω_{0j}, and a width, γ_j, that is inversely related to the excitation lifetime. This functional form is attributed to samples with homogeneous broadening, where the width of the Raman band is related to the damping coefficient γ_j.[37] The other functional form is that of Gaussians

$$\chi''(\omega) = C + \sum_j^n I_{0j} e^{-(\omega - \omega_{oj})^2/\sigma_j^2}, \tag{4}$$

where I_{0j}, ω_{oj}, and σ_j are the height, center frequency, and statistical width of each band, and C is a constant. The Gaussian functional form is used for inhomogeneous broadening, where the width of a band is due to a statistical distribution of the resonant frequency ω_{0j}. The $\chi''(\omega)$ of each sample was fitted to the form in Eqs. (3) and (4), by using a least-squares minimization method. For each fit, all parameters for all modes were allowed to vary simultaneously. Figures 2 and 3 show the Lorentzian and Gaussian fits for all four samples and show the individual oscillators from the fit. BZN shows nine features in its spectrum, and therefore nine oscillators were used for the Lorentzian fit. For the other samples, nine oscillators were enough to fit the spectrum, although the fit for BMN showed that eight oscillators were enough and that a ninth oscillator was unnecessary (the introduction of the new oscillator yielded a very weak amplitude for this mode). For the Gaussian fits, the constant C was necessary to fit the remaining intensity at high frequencies. The Gaussian function has been used to fit the Raman spectrum of BZN previously in the literature.[9] For our fits to the Raman susceptibility, although the Gaussian function seems to produce a good fit, the fit did not always converge to the same parameters. Furthermore, the Lorentzian function produced a better fit in the 300–600 cm^{-1} region. For the rest of this paper, we will use the parameters extracted from the Lorentzian fittings. The extracted damping coefficient for each mode, γ_j, will also be used for comparison to the damping coefficients obtained from the IR of the low-frequency modes. Table I shows the parameters obtained from the Lorentzian function fit to the Raman susceptibility.

A factor group analysis of the ideal pyrochlore structure yields six Raman-active modes (R), seven IR modes, and one F_{1u} acoustic mode[38]

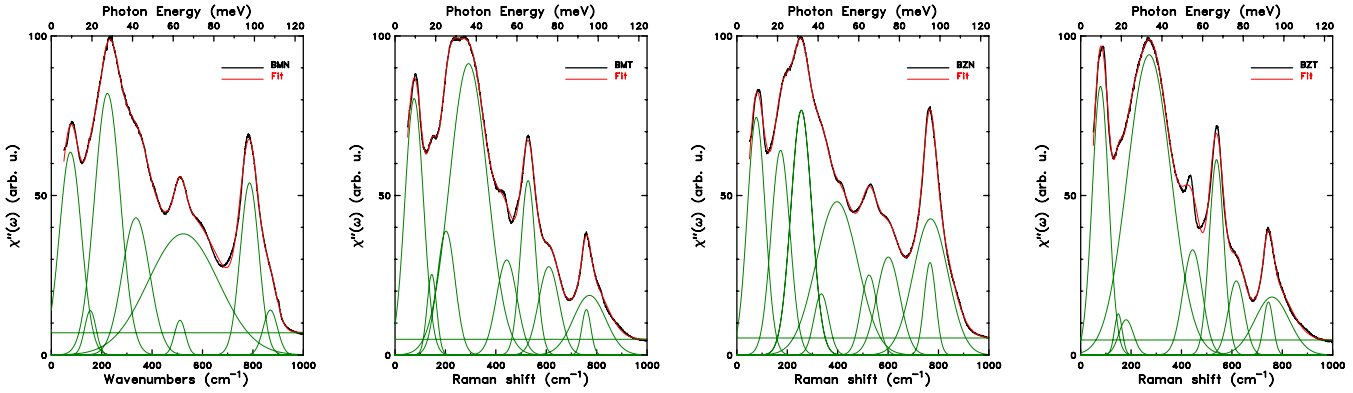

FIG. 3. (Color online) Gaussian fit to the imaginary part of the Raman susceptibility (left to right: BMN, BMT, BZN, and BZT). The figure shows the data (black), the fitting (red), and the individual functions (green) from the fit.

TABLE I. Parameters for BMN, BMT, BZN, and BZT from the Lorentzian fitting $\Sigma A_j/[1+4(\omega-\omega_{oj})^2/\gamma_j^2]$.

BMN			BMT			BZN			BZT		
Integrated intensity (arb. u.)	ω_{oj} (cm^{-1})	γ_j (cm^{-1})	Integrated intensity (arb. u.)	ω_{oj} (cm^{-1})	γ_j (cm^{-1})	Integrated intensity (arb. u.)	ω_{oj} (cm^{-1})	γ_j (cm^{-1})	Integrated intensity (arb. u.)	ω_{oj} (cm^{-1})	γ_j (cm^{-1})
68	73	104	32	74	86	61	77	88	30	79	76
7	164	72	3	148	38	47	180	98	1	158	34
100	230	142	23	216	96	100	256	124	9	208	102
85	346	190	100	297	200	47	342	122	100	281	210
			3	430	44	24	420	104	6	434	48
28	511	92	26	529	80	46	526	116	22	540	67
33	599	146	8	620	78	28	610	120	4	624	62
69	786	94	8	758	50	75	766	88	7	744	48
5	860	62	9	801	114	11	830	96	8	789	118

$$\Gamma = A_{1g}(R) + E_g(R) + 4F_{2g}(R) + 7F_{1u}(\mathrm{IR}) + F_{1u} + 4F_{2u} + 2F_{1g} + 3A_{2u} + 3E_u, \quad (5)$$

where all six Raman modes involve only motion of oxygen atoms. Each mode was studied and assigned by first referencing the literature on diverse samples with structures close to the ideal pyrochlore structure.[10,12–29] Then, the bands were also compared to our *ab initio* calculations for $Bi_2Ti_2O_7$ and those in the literature for $Cd_2Nb_2O_7$.[11] Table II shows the frequencies of the various observed modes for the four samples along with their assignment. We discuss in the following sections each mode and its assignment.

TABLE II. The Raman modes of BMN, BMT, BZN, and BZT are shown along with their tentative assignment. The frequencies calculated for $Bi_2Ti_2O_7$ from first principles are also reported. The superscript *i* refers to an unstable mode. The data and assignments for $Cd_2Nb_2O_7$ are taken from Fischer's computational work (Ref. 11). The rationale for the assignment of each mode is discussed in the text.

Raman frequencies (cm^{-1})						
BMN	BMT	BZN	BZT	$Bi_2Ti_2O_7$	$Cd_2Nb_2O_7$ (Ref. 11)	Tentative assignment
73	74	77	74	F_{1u}:86	F_{1u}:71	F_{1u}
164	148	180	158	F_{1u}:142^i	E_u:133	F_{1u}
					F_{1u}:190	
230	216	256	208	F_{2g}:262	F_{2g}:265	F_{2g}
346	297	342	281	E_g:281	E_g:302	E_g+F_{2g}
					F_{2g}:332	
419	430	420	434	F_{2g}:395	F_{2g}:441	F_{2g}
511	529	526	540	A_{1g}:535	A_{1g}:482	A_{1g}
599	620	610	624	F_{2g}:537	F_{1g}:617	F_{2g}
786	758	766	744	F_{2g}:711		Overtone?
860	801	830	789		F_{2g}:880	Overtone?

B. Low-frequency modes (70–180 cm^{-1}). Relaxation of the selection rules

All four samples showed bands from 70 to 180 cm^{-1}. These modes are lower in frequency than those observed for many pyrochlores. For various *A* and *B* substituents, the lowest frequency Raman mode attributed to a symmetry allowed vibration is at 220 cm^{-1}. A few examples are (with many other pyrochlores contained in the references): 220 cm^{-1} for $Yb_2Ti_2O_7$,[12] 230 cm^{-1} for $Pb_2Sb_2O_7$,[24] 236 cm^{-1} for $Gd_2Ti_2O_7$,[12] ~240 cm^{-1} for $Cd_2Re_2O_7$,[19] 289 cm^{-1} for $Tl_2Mn_2O_7$,[13] 292 cm^{-1} for $In_2Mn_2O_7$,[13] 298 cm^{-1} for $La_2Zr_2O_7$,[27] 302 cm^{-1} for $Y_2Mn_2O_7$,[12] 303 cm^{-1} for $Nd_2Ir_2O_7$,[17] 306 cm^{-1} for $Nd_2Hf_2O_7$,[27] 308 cm^{-1} for $Sm_2Sn_2O_7$,[16] and 312 cm^{-1} for both $Yb_2Sn_2O_7$ and $Lu_2Sn_2O_7$.[16] Since all Raman-active modes only involve motion of oxygen atoms, the high mass of the Bi cation should not be responsible for lower frequencies. Such low-frequency modes would suggest much weaker *A*-O or O-*A*-O force constants for Bi than for all the compounds referenced above. For other bismuth pyrochlores, the lowest modes are around 250 cm^{-1} for $Bi_2Hf_{2-x}Ti_{2x}O_7$,[18] and 226 cm^{-1} for various $Bi_xY_{(2-x)}Ti_2O_7$.[14] For BZN, the 180 cm^{-1} band has been reported in the literature but its assignment seems difficult. It has been explained as the splitting of an F_{2g} mode, where one band belongs to a Bi-O stretch at 180 cm^{-1} and the other to a Zn-O stretch at 251 cm^{-1}.[8] However, the calculations for the splitting of this mode includes the masses of the Bi and Zn cations. In contrast, other work has assigned it to a F_{2g} mode separate from the 255 cm^{-1} F_{2g} mode.[39]

We propose an alternative assignment. We propose that the band in the 150–180 cm^{-1} region is a normally Raman-inactive, but IR-active F_{1u} mode, that appears in the Raman spectra due to the displacive disorder of the *A* site in the Bi pyrochlores. We can recall that, based on symmetry, the selection rules result in some vibrational modes being optically inactive.[40] Random displacement disorder can result in the relaxation of the selection rules, and we can expect previously inactive modes to appear in both IR and Raman spectra, and IR only modes in the Raman and vice versa. In the 150–180 cm^{-1} region, the infrared data shows bands with

TABLE III. The infrared modes with close frequencies to those of the Raman are shown. [From Chen *et al.* (Ref. 7)] * denotes that Chen assigns this mode to O-*A*-O bending. ** denotes that the highest frequency mode is assigned to a shorter *A*-O′ bond.

IR frequencies (cm^{-1})				
BMN	BMT	BZN	BZT	Mode assignment
86	83		81	F_{1u}: O′-*A*-O′ Bend
	149	142	145	F_{1u}: O-*A*-O Bend
178*	178	178	192	F_{1u}: *A*-BO_6 Stretch
291	295	259	268	F_{1u}: O-*B*-O Bend
367	295	340	303	F_{1u}: *A*-O Stretch
599	642	624	639	F_{1u}: *B*-O Stretch
850		850		F_{1u}: *A*-O′ Stretch**

very close frequencies to those reported here for the Raman. (Compare Tables II and III.) The attribution of these modes to the relaxation of the selection rules is also consistent with *ab initio* calculations for $Bi_2Ti_2O_7$, which predict the lowest F_{2g} mode at 262 cm^{-1}. The assignment is also consistent with similar calculations for $Cd_2Nb_2O_7$ by Fischer *et al.*[11] which predict the lowest F_{2g} mode at 265 cm^{-1} and an F_{1u} mode at 190 cm^{-1}.

The damping coefficients for the Raman modes around 180 cm^{-1} obtained from the fit in Eq. (3) were compared to those from the IR data of Chen *et al.*[7] The IR analysis used a Lorentzian oscillator model for the susceptibility, which also uses a damping coefficient γ_j

$$\chi(\omega) = \sum_j^n \frac{\omega_{pj}^2}{(\omega_{oj}^2 - \omega^2) - i\omega\gamma_j} \quad \text{(IR)}. \tag{6}$$

The imaginary part of each term in Eq. (6) approaches a Lorentzian function in Eq. (3) when $\omega \approx \omega_{0j}$ and $\gamma_j \ll \omega_{0j}$. We compared the damping coefficients of the 150–180 cm^{-1} modes, extracted from the Lorentzian fit and listed in Table I, to the damping coefficients from the IR. (Tables I–IV of Ref. 7). The comparison suggests that the 150–180 cm^{-1} IR and Raman bands arise from the same vibration. It should be mentioned that Rayleigh scattering could add an unknown to this region of the Raman spectrum and affect the fit. Nonetheless, the parameters from the Raman fits yielded values close to the IR and the comparison is worth mentioning. Specifically, for BZN, the 180 cm^{-1} mode had damping coefficients of 88 cm^{-1} for the Raman and 84 cm^{-1} for the IR. For BZT, the widths of the mode near 150 cm^{-1} were also close (32 and 34 cm^{-1}). BMT has center frequencies for the Raman and IR that are nearly identical (148 and 149 cm^{-1}) and the widths are close (35and 38 cm^{-1}). As for BMN, the weak mode at 164 cm^{-1} is closest to the 178 cm^{-1} in the IR, and their widths are 72 cm^{-1} for the Raman and 84 cm^{-1} for the IR.

All four bismuth pyrochlores show a feature in the Raman spectra around 80 cm^{-1} (Fig. 1). This mode has also been observed in BZN by Wang *et al.*[41] The *ab initio* calculations for $Bi_2Ti_2O_7$ predict an F_{1u} mode around 86 cm^{-1} that is consistent with the IR data. And, the calculations for $Cd_2Nb_2O_7$ by Fischer *et al.*[11] predict an IR F_{1u} mode around 71 cm^{-1}, and an optically inactive E_u mode at 69 cm^{-1}. Therefore, we have assigned this mode to a normally Raman-inactive mode. After correcting for the Bose factor and fitting the data, the mode in our four samples had a center frequency about 70 cm^{-1}. This is relatively close to IR modes near 80 cm^{-1}.[7] However, the fitting was not as reliable for the Raman since the data was available only above 50 cm^{-1}. Furthermore, Rayleigh scattering in this region can also affect the fit. In summary, the similarity of the low-frequency Raman bands to IR modes, and the agreements with *ab initio* calculations on the pyrochlores $Bi_2Ti_2O_7$ and $Cd_2Nb_2O_7$, suggest that these low-frequency modes arise from the relaxation of selection rules.

C. 200–400 cm^{-1} bands

The frequency of the band attributed to the lowest frequency F_{2g} mode varies significantly for pyrochlores. This mode is assigned to a band around 200–240 cm^{-1} for various titanates,[10,22] 250 cm^{-1} for $Cd_2Re_2O_7$,[19] and 300–310 cm^{-1} for some manganates[12,13] and stannates.[28] For other niobates and tantalates, this mode is at 245 cm^{-1} for $Cd_2Ta_2O_7$,[29] and 279 cm^{-1} in $Cd_2Nb_2O_7$.[11] Table II shows the frequencies of this mode for our bismuth samples. The proximity of the frequency of this band to that of other pyrochlores makes the F_{2g} assignment the most reasonable. In the literature, the band assigned to E_g also has significantly varying frequencies: 294 cm^{-1}, 297 cm^{-1}, 300 cm^{-1}, 310 cm^{-1}, 327 cm^{-1}, 330 cm^{-1}, 331 cm^{-1}, 340 cm^{-1}, 346 cm^{-1}, 350 cm^{-1}, 379 cm^{-1}, and 405 cm^{-1}, for $Nd_2Mb_2O_7$,[26] $BiYTi_2O_7$,[14] $Cd_2Re_2O_7$,[19] $Y_2Ti_2O_7$,[14] $Tl_2Mn_2O_7$,[13] $Tb_2Ti_2O_7$,[21] $Er_2Ti_2O_7$,[22] $La_2Sn_2O_7$,[16] $In_2Mn_2O_7$,[13] $Pb_2Sb_2O_7$,[24] $Lu_2Sn_2O_7$,[16] and $La_2Zr_2O_7$,[27] respectively. This is a variance of 10% for the samples mentioned. Our calculations for $Bi_2Ti_2O_7$ predict the E_g mode around 281 cm^{-1}. Fischer's calculations for $Cd_2Nb_2O_7$ offer further insight into this band.[11] They estimate 300 cm^{-1} for the E_g mode but they also predict an additional F_{2g} mode at 332 cm^{-1}. The large width of the Raman band, as seen in Fig. 2 would suggest that the E_g and F_{2g} modes were not resolved in our spectra. It should be noted that this is the only major difference between our calculations for $Bi_2Ti_2O_7$ and those of Fischer for $Cd_2Nb_2O_7$. Our calculations for $Bi_2Ti_2O_7$ do not show a mode near E_g but instead near the A_{1g} mode. Interestingly, our calculations for $Bi_2Ti_2O_7$ also yield an F_{1u} mode at 262 cm^{-1},[36] which is also observed in the IR.[7] Due to the relaxation of the selection rules, we must consider that the IR and Raman spectra may show the same vibration. This analysis would explain the trend, also present in the IR, of higher frequencies observed for the lighter *B* cation in BZN and BMN, than for BMT and BZT. However, based on Fischer's calculations, and the proximity of an F_{2g} mode to the E_g mode in other pyrochlores,[10,12–14,19–22,25,26,28,29] we have assigned the ~300 cm^{-1} feature in the Raman spectrum to the E_g mode and one of the F_{2g} modes.

D. 400–600 cm^{-1} bands: A_{1g} and F_{2g}

The A_{1g}, and one of the F_{2g} modes of the ideal structure are assigned to bands at 530 cm^{-1} and 420 cm^{-1}, respectively. These modes are mostly due to vibrations of the BO_6 octahedra, as found by lattice dynamic calculations on other pyrochlores.[12,27,28,42] Unlike the E_g mode, the frequency of the A_{1g} mode does not vary greatly for different pyrochlores: 488 cm^{-1}, 489 cm^{-1}, 495 cm^{-1}, 498 cm^{-1}, 500 cm^{-1}, 510 cm^{-1}, 510 cm^{-1}, 512 cm^{-1}, 513 cm^{-1}, 520 cm^{-1}, 523 cm^{-1}, and 525 cm^{-1}, for $Nd_2Mb_2O_7$,[26] $Tl_2Mn_2O_7$,[13] $La_2Sn_2O_7$,[16] $La_2Zr_2O_7$,[27] $Cd_2Re_2O_7$,[19] $In_2Mn_2O_7$,[13] $Lu_2Sn_2O_7$,[16] $Tb_2Ti_2O_7$,[21] $Pb_2Sb_2O_7$,[24] $BiYTi_2O_7$,[14] $Y_2Ti_2O_7$,[14] and $Er_2Ti_2O_7$,[22] respectively. This is a variance of less than 3%. The frequency of the A_{1g} mode is remarkably constant despite all the different substituents mentioned above. For our samples, the frequencies of this mode agree with other pyrochlores and also agree well with our calculations for $Bi_2Ti_2O_7$.

The A_{1g} mode can give insight into the force constants of the pyrochlore structure. According to the lattice-dynamical calculations by Vanderborre[27] and Brown,[12] the A_{1g} mode is mainly due to the vibration of the BO_6 octahedra. The main contribution to the frequency of this mode comes from force constants related to O-*B*-O bending (~80% of the potential-energy distribution).[12] Based on the strong agreement in the A_{1g} frequency of so many different pyrochlores, and the characterization of this vibration by Vanderborre and Brown, we expect the force constants responsible to be similar for pyrochlores. This is the case for many titanates[10] and manganates,[12] where the bending force constants for the two O-*B*-O bends are reported around 0.4 and 0.3 N cm^{-1}. Therefore, it is reasonable to expect our samples to have similar O-*B*-O force constants. Comparing the Nb samples to the Ta samples, there was a 3% systematic increase in frequency for the A_{1g} mode for BMT over BMN and BZT over BZN. This result corroborates the suggestion that oxygen binds more tightly to Ta than to Nb in the octahedron.[8] The Raman band around 430 cm^{-1} also has similar frequencies to other pyrochlores.[13,14,16,19,21,22,24,26] This mode is attributed mostly to the *B*-O stretch force constant.[12,13,27] The fact that the Ta samples shows higher frequencies for this mode also suggests stronger force constants in the octahedra for BZT and BMT than for BZN and BMN.

E. High-frequency modes (600–900 cm^{-1})

The Raman spectra of all four samples show bands around 620 and 780 cm^{-1}. We will begin our discussion with the 620 cm^{-1} band. The highest frequency band assigned to an F_{2g} mode for various pyrochlores is around 600 cm^{-1}, a few examples are: 590 cm^{-1} ($Yb_2Ti_2O_7$),[10] 590 cm^{-1} ($La_2Zr_2O_7$),[27] 598 cm^{-1} ($Er_2Mn_2O_7$),[12] 618 cm^{-1} ($Nd_2Ir_2O_7$),[17] and 620 cm^{-1} ($Lu_2Sn_2O_7$).[16] These frequencies are in good agreement for such different substituents.[10] However, this 600 cm^{-1} mode is not observed in single crystals of the pyrochlores $Cd_2Re_2O_7$,[19] and $Nd_2Mo_2O_7$.[26] The *ab initio* calculations by Fischer predict a mode at 617 cm^{-1} but with an F_{1g} symmetry (optically inactive) instead of an F_{2g} symmetry.[11] For some titanates, there is a mode near 550 cm^{-1} assigned to F_{2g} while the mode around 610 cm^{-1} is associated with an impurity phase due to rutile TiO_2.[15,22,25] Our calculations for $Bi_2Ti_2O_7$ predict an F_{2g} mode around 535 cm^{-1}. For the samples studied here, the assignment of the modes becomes further problematic in that the IR also shows modes with frequencies very close to those in the Raman. (See Tables II and III.) Perhaps, the strongest evidence to assign this mode to any type of symmetry are the studies on single crystal $Dy_2Ti_2O_7$ by Mkączka *et al.*[23] These polarization-dependent studies on a single crystal show that the 580 cm^{-1} mode has an F_{2g} symmetry.

The mode around 620 cm^{-1} was also observed with higher frequencies for the Ta samples compared to the Nb samples. The higher frequency F_{2g} mode is mostly attributed to the *B*-O force constant in the octahedron by Vanderborre for different stannates and titanates,[28] and attributed to O-*B*-O bending force constants for manganates by Brown *et al.*[12,13] This mode also corroborates that the force constants of the BO_6 octahedron are comparable for the Bi pyrochlores to other pyrochlores and that they are slightly larger for the Ta samples. If we consider the possibility that this mode is a normally Raman-silent F_{1g} mode, the conclusion for the force constants remains the same.

Perhaps the most interesting mode in our data is at 780 cm^{-1}. Modes with such high frequency are usually assigned as combination bands or overtones. For example, $Tb_2Ti_2O_7$ shows a weak band at around 670 cm^{-1} but the mode is assigned as an overtone by stating that the highest frequency F_{2g} mode should not exceed 600 cm^{-1},[21] in reference to lattice-dynamical calculations by Gupta *et al.*[10] for other titanates. In contrast, *ab initio* calculations by Fischer predict a F_{2g} mode with a frequency as high as 880 cm^{-1}.[11] And, our calculations for $Bi_2Ti_2O_7$ predict an F_{2g} mode at 711 cm^{-1}. In BZN, this mode has been previously attributed to an overtone[39] and also to a stretching of the Nb-O bond.[8] For BZN, no physical process has been suggested to be responsible for the high amplitude of this mode. Normally, a two phonon-scattering process is expected to have a much lower probability than a first-order process. Physical processes such as resonant raman scattering, where the incident laser frequency is close to a resonance in the material, can greatly increase the amplitude of an overtone or combination band. Strong anharmonic coupling can also lead to the appearance of combination and overtone bands.[43] There is no strong resonance in this region for our Bi pyrochlore samples and the high amplitude observed for this mode for different laser frequencies suggests it is not a resonant scattering process. Strong anharmonicity could explain the high amplitude of an overtone but our current set of data cannot offer insight into this suggestion.

The mode near 780 cm^{-1} shows interesting trend for our samples. The mode in the Nb samples has a higher frequency than the Ta samples. If this mode is a fundamental Raman-active mode and the BO_6 force constants are higher for Ta samples than for Nb samples, then we expect the opposite. We can explore the possibility of an optically inactive mode where the *B* cation moves as well as the oxygen. To estimate, let us consider a vibrational mode with a reduced mass of

$$\mu = \frac{m_B \times 6m_O}{m_B + 6m_O}, \tag{7}$$

to predict the frequency ratio

$$\frac{\omega_{\mathrm{Nb}}^2}{\omega_{\mathrm{Ta}}^2} = \frac{k_{\mathrm{Nb}}}{k_{\mathrm{Ta}}} \frac{\mu_{\mathrm{Ta}}}{\mu_{\mathrm{Nb}}}. \tag{8}$$

A force-constant ratio $k_{\mathrm{Nb}}/k_{\mathrm{Ta}}$ of 0.91, as reported by Wang *et al.*,[39] yields a ratio $\omega_{\mathrm{Nb}}/\omega_{\mathrm{Ta}}$ of 1.03. This is indeed in good agreement with our results, (see Table II), and consistent with a suggestion that this band is a normally Raman-inactive mode that involves the motion of *B* cations (or the overtone of such a mode). In summary, the high amplitude and high frequency of this mode, as well as the difference in predictions from lattice dynamical and *ab initio* calculations, make the assignment of this mode difficult. Future work on the synthesis of single crystals would make the assignment of this mode more clear. This was the case for $Dy_2Ti_2O_7$ single crystals, where it was showed that all the modes above 590 cm^{-1} have A_{1g} symmetry and the modes are attributed to overtones.[23] Also, more *ab initio* calculations for other pyrochlores would greatly benefit the study of this region of the spectrum. If the mode is indeed an overtone, it would be interesting to explore why the *ab initio* calculations for both $Cd_2Nb_2O_7$ and $Bi_2Ti_2O_7$ seem to agree well with experiment on most of the Raman modes, but overestimate the highest frequency mode.

Lastly, very weak bands around 800 cm^{-1} were observed for all samples. These high-frequency modes have been attributed to unequal lengths for the *A*-O′ bond in the A_2O' substructure.[44] However, the *ab initio* calculations by Fischer *et al.* suggest the higher frequency F_{2g} mode may be in this spectral region.

IV. CONCLUSIONS

The Raman spectra of a family of pyrochlores, BMN, BMT, BZN, and BZT, are very similar, suggesting no major structural differences among these materials. The spectra of these four samples agree well with *ab initio* calculations[36] on $Bi_2Ti_2O_7$ and those found in the literature[11] for the niobate $Cd_2Nb_2O_7$. The modes were assigned by comparison to other pyrochlores structured materials, *ab initio* calculations, and lattice-dynamical calculations found in the literature. The comparison to other pyrochlores suggested comparable force constants for the BO_6 octahedron. All samples showed modes that can be attributed to relaxation of the selection rules and therefore showed the reduction in symmetry of these samples due to the displacive disorder. This attribution was corroborated by comparison to the IR spectra and *ab initio* calculations in the literature. Finally, comparison of the Raman spectra shows that the Ta samples have stronger force constants for the BO_6 octahedron than the Nb samples.

ACKNOWLEDGMENTS

This work was supported in part by the NSF under Grant No. DMR-0449710 and the DOE under Grants No. DE-AI02-03ER46070 and No. DE-FG02-02ER45984. Work at UNF was supported by the National Science Foundation under Grant No. DMR-0805073, Research Corporation Cottrell College Science under Award No. CC 6130, Petroleum Research Fund under Award No. 40926-GB10, and Office of Naval Research (ONR) under Award No. N00014-06-1-0133. Work at Trinity College was partly funded by Science Foundation Ireland under Grant No. RFP/09/MTR/2295. D.J.A also thanks Greg Wurtz and Michael Lufaso for invaluable discussions.

[1] G. I. Golovshchikova, V. A. Isupov, A. G. Tutov, I. E. Mylnikova, P. A. Nikitnia, and O. I. Tulinova, Sov. Phys. Solid State **14**, 2539 (1973).
[2] M. Lanagan, D. Anderson, A. Baker, J. Nino, S. Perini, C. A. Randall, T. R. Strout, T. Sogabe, and H. Youn, in *Proceedings of the International Symposium on Microelectronics*, edited by J. Graves (Baltimore, MD, 2001), p. 155.
[3] A. W. Sleight, Inorg. Chem. **7**, 1704 (1968).
[4] I. Levin, T. G. Amos, J. C. Nino, T. A. Vanderah, C. A. Randall, and M. T. Lanagan, J. Solid State Chem. **168**, 69 (2002).
[5] T. A. Vanderah, I. Levin, and M. W. Lufaso, Eur. J. Inorg. Chem. **2005**, 2895 (2005).
[6] M. Avdeev, M. K. Haas, J. D. Jorgensen, and R. J. Cava, J. Solid State Chem. **169**, 24 (2002).
[7] M. Chen, D. B. Tanner, and J. C. Nino, Phys. Rev. B **72**, 054303 (2005).
[8] H. Wang, H. Du, and X. Yao, Mater. Sci. Eng., B **99**, 20 (2003).
[9] S. Kamba, V. Porokhonskyy, A. Pashkin, V. Bovtun, J. Petzelt, J. C. Nino, S. Trolier-McKinstry, M. T. Lanagan, and C. A. Randall, Phys. Rev. B **66**, 054106 (2002).
[10] H. C. Gupta, S. Brown, N. Rani, and V. B. Gohel, J. Raman Spectrosc. **32**, 41 (2001).
[11] M. Fischer, T. Malcherek, U. Bismayer, P. Blaha, and K. Schwarz, Phys. Rev. B **78**, 014108 (2008).
[12] S. Brown, H. C. Gupta, J. A. Alonso, and M. J. Martinez-Lope, J. Raman Spectrosc. **34**, 240 (2003).
[13] S. Brown, H. C. Gupta, J. A. Alonso, and M. J. Martinez-Lope, Phys. Rev. B **69**, 054434 (2004).
[14] A. Garbout, A. Rubbens, R. Vannier, S. Bouattour, and A. W. Kolsi, J. Raman Spectrosc. **39**, 1469 (2008).
[15] A. Garbout, S. Bouattour, and A. W. Kolsi, J. Alloys Compd. **469**, 229 (2009).
[16] H. C. Gupta, S. Brown, N. Rani, and V. B. Gohel, Int. J. Inorg. Mater. **3**, 983 (2001).
[17] T. Hasegawa, N. Ogita, K. Matsuhira, S. Takagi, M. Wakeshima, Y. Hinatsu, and M. Udagawa, J. Phys.: Conf. Ser. **200**, 012054 (2010).
[18] S. J. Henderson, O. Shebanova, A. L. Hector, P. F. McMillan, and M. T. Weller, Chem. Mater. **19**, 1712 (2007).
[19] C. S. Knee, J. Holmlund, J. Andreasson, M. Kall, S. G. Eriksson, and L. Borjesson, Phys. Rev. B **71**, 214518 (2005).
[20] T. T. A. Lummen, I. P. Handayani, M. C. Donker, D. Fausti, G.

Dhalenne, P. Berthet, A. Revcolevschi, and P. H. M. van Loosdrecht, Phys. Rev. B **77**, 214310 (2008).
[21] M. Mączka, M. L. Sanjuán, A. F. Fuentes, K. Hermanowicz, and J. Hanuza, Phys. Rev. B **78**, 134420 (2008).
[22] M. Mączka, J. Hanuza, K. Hermanowicz, A. F. Fuentes, K. Matsuhira, and Z. Hiroi, J. Raman Spectrosc. **39**, 537 (2008).
[23] M. Mączka, M. L. Sanjuán, A. F. Fuentes, L. Macalik, J. Hanuza, K. Matsuhira, and Z. Hiroi, Phys. Rev. B **79**, 214437 (2009).
[24] F. Rosi, V. Manuali, C. Miliani, B. G. Brunetti, A. Sgamellotti, T. Grygar, and D. Hradil, J. Raman Spectrosc. **40**, 107 (2009).
[25] S. Saha, S. Singh, B. Dkhil, S. Dhar, R. Suryanarayanan, G. Dhalenne, A. Revcolevschi, and A. K. Sood, Phys. Rev. B **78**, 214102 (2008).
[26] K. Taniguchi, T. Katsufuji, S. Iguchi, Y. Taguchi, H. Takagi, and Y. Tokura, Phys. Rev. B **70**, 100401 (2004).
[27] M. T. Vanderborre, E. Husson, and H. Brusset, Spectrochim. Acta, Part A **37**, 113 (1980).
[28] M. T. Vanderborre, E. Husson, J. P. Chatry, and D. Michel, J. Raman Spectrosc. **14**, 63 (1983).
[29] M. T. Vandenborre and E. Husson, J. Solid State Chem. **50**, 362 (1983).
[30] J. C. Nino, M. T. Lanagan, and C. A. Randall, J. Mater. Res. **16**, 1460 (2001).
[31] D. J. Dunstan and M. D. Frogley, Rev. Sci. Instrum. **73**, 3742 (2002).
[32] J. P. Perdew and Y. Wang, Phys. Rev. B **45**, 13244 (1992).
[33] R. Dovesi, V. R. Saunders, C. Roetti, R. Orlando, C. M. Zicovich-Wilson, F. Pascale, B. Civalleri, K. Doll, N. M. Harrison, I. J. Bush, P. D'Arco, and M. Llunell, CRYSTAL06 *User's Manual* (University of Torino, Torino, 2007).
[34] B. B. Hinojosa, J. C. Nino, and A. Asthagiri, Phys. Rev. B **77**, 104123 (2008).
[35] C. J. Fennie, R. Seshadri, and K. M. Rabe, arXiv:0712.1846 (unpublished).
[36] C. H. Patterson, Phys. Rev. B **82**, 155103 (2010).
[37] J. McHale, *Molecular Spectroscopy* (Prentice-Hall, Englewood Cliffs, 1999).
[38] R. A. McCauley, J. Opt. Soc. Am. **63**, 721 (1973).
[39] Q. Wang, H. Wang, and X. Yao, J. Appl. Phys. **101**, 104116 (2007).
[40] D. A. Long, *Raman Spectroscopy* (McGraw-Hill International Book, New York, 1977), p. 65.
[41] H. Wang, S. Kamba, H. Du, M. Zhang, C.-T. Chia, S. Veljko, S. Denisov, F. Kadlec, J. Petzelt, and X. Yao, J. Appl. Phys. **100**, 014105 (2006).
[42] H. C. Gupta and S. Brown, J. Phys. Chem. Solids **64**, 2205 (2003).
[43] B. N. Ganguly, R. D. Kirby, M. V. Klein, and G. P. Montgomery, Phys. Rev. Lett. **28**, 307 (1972).
[44] R. L. Withers, T. R. Wellberry, A. K. Larsson, Y. Liu, L. Noren, H. Rundlof, and F. J. Brink, J. Solid State Chem. **177**, 231 (2004).